



# Combined calorimetric gas- and spore-based biosensor array for online monitoring and sterility assurance of gaseous hydrogen peroxide in aseptic filling machines

Julio Arreola<sup>a,b</sup>, Michael Keusgen<sup>b</sup>, Torsten Wagner<sup>a,c</sup>, Michael J. Schöning<sup>a,c,\*</sup>

<sup>a</sup> Institute of Nano- and Biotechnologies (INB), Aachen University of Applied Sciences, Campus Jülich, 52428, Jülich, Germany

<sup>b</sup> Institute of Pharmaceutical Chemistry, Philipps-University Marburg, Marbacher Weg 6-10, 35032 Marburg, Germany

<sup>c</sup> Institute of Complex Systems 8 (ICS-8), Research Centre Jülich GmbH, 52425, Jülich, Germany

## ARTICLE INFO

### Keywords:

Biosensor  
Sterilization  
Spore  
Hydrogen peroxide  
Aseptic filling machine

## ABSTRACT

A combined calorimetric gas- and spore-based biosensor array is presented in this work to monitor and evaluate the sterilization efficacy of gaseous hydrogen peroxide in aseptic filling machines. H<sub>2</sub>O<sub>2</sub> has been successfully measured under industrial conditions. Furthermore, the effect of H<sub>2</sub>O<sub>2</sub> on three different spore strains, namely *Bacillus atrophaeus*, *Bacillus subtilis* and *Geobacillus stearothermophilus*, has been investigated by means of SEM, AFM and impedimetric measurements. In addition, the sterilization efficacy of a spore-based biosensor and the functioning principle are addressed and discussed: the sensor array is convenient to be used in aseptic food industry to guarantee sterile packages.

## 1. Introduction

Aseptic filling machines are broadly employed in biomedical and food industry to provide sterilized liquid products. In these machines, the entire aseptic processing is performed, including the sterilization of the packing material, filling and sealing of the product. Maintaining sterile aseptic packaging is a crucial aspect to assure the shelf life and safety of the goods. A wide range of sterilization methods is available for this purpose, for instance heat, hydrogen peroxide and UV or plasma radiation (Ansari and Datta, 2003). Among them, chemical methods in form of gases are extensively used such as ethylene oxide, formaldehyde, peracetic acid or gaseous hydrogen peroxide (H<sub>2</sub>O<sub>2</sub>). Although all of them have been employed to sterilize packaging materials, not all are optimal for aseptic processing; ethylene oxide and formaldehyde are carcinogenic (Koda et al., 1999). Peracetic acid is a mixture formed from acetic acid and hydrogen peroxide; upon decomposition, it forms acetic acid and water. Since its vapor is very pungent and irritating, residuals may cause unwanted flavors in some food products (Toledo, 1988). As a result, H<sub>2</sub>O<sub>2</sub> has become a popular choice as a sterilant for aseptic filling machines. H<sub>2</sub>O<sub>2</sub> has the best safety profile in comparison to other sterilization gases (Johnston et al., 2005), mainly because it breaks down into water and oxygen, leaving virtually no residues and therefore being eco-friendly. In addition, its strong oxidation properties are capable of killing an extensive amount of microorganisms, for example, viruses, bacteria, spores and fungi

(Heckert et al., 1997; Kitancharoen et al., 1997; Otter and French, 2009; Swartling and Lindgren, 1968). The effectiveness of H<sub>2</sub>O<sub>2</sub> is primarily affected by its exposure time, temperature and concentration.

Microbiological methods are the standard approach to evaluate the efficacy of sterilization systems with gaseous hydrogen peroxide. Here, the packaging is artificially inoculated with microbiological spores, which are extremely resistant to the sterilization agent. Subsequently, the inoculated packing is exposed to the sterilant and finally incubated for a certain amount of time. After that, the viability of the spores is determined either by counting the surviving spores before and after sterilization (count-reduction test) or by determining the relationship between the number of non-sterile and sterile packages (end-point test) (Cerny, 1992). Although these methods are reliable and widespread, they lack rapid output responses (48–72 h) and they are cumbersome.

Over the last few years, more sophisticated methods have been developed by the integration of sensor technologies to determine, for instance, hydrogen peroxide concentrations or the viability of spores. Gaseous H<sub>2</sub>O<sub>2</sub> detection has been broadly reported in literature by means of electrochemical (Kulys, 1992), acoustic (Liu et al., 2011), conductometric (Verma et al., 2011), colorimetric (Xu et al., 2011) or calorimetric measurements (Kirchner et al., 2011). Some of them are not suitable for online- and inline monitoring in aseptic filling machines (electrochemical, colorimetric), because of the lack of portability of the measuring equipment or sophisticated sample preparation (solution-based). Other methods have high response times (> 30 s) in comparison to

\* Corresponding author. Institute of Nano- and Biotechnologies (INB), Aachen University of Applied Sciences, Campus Jülich, 52428, Jülich, Germany.  
E-mail address: [schoening@fh-aachen.de](mailto:schoening@fh-aachen.de) (M.J. Schöning).

standard industrial  $\text{H}_2\text{O}_2$  exposure times ( $< 2$  s) or may not be able to handle high temperatures (up to  $300^\circ\text{C}$ ). Moreover, calorimetric gas sensors have been previously introduced (Kirchner et al., 2011; Näther et al., 2009; Oberländer et al., 2014) to overcome these limitations for applications in aseptic food industry. They incorporate a differential setup of two temperature-sensitive structures: one of them is passivated by an inert polymer layer and functions as a reference, whereas the other one is catalytically activated by manganese oxide ( $\text{MnO}_2$ ). When gaseous  $\text{H}_2\text{O}_2$  is in contact with the sensor surface, only where the catalyst is located, hydrogen peroxide is split into oxygen and water, and the other part of the sensor remains inert. As a result, an exothermic reaction and therefore an increase of temperature particularly on the active side of the sensor occurs. At the end, the temperature difference can be correlated quantitatively to the  $\text{H}_2\text{O}_2$  concentration.

However, the measurement of  $\text{H}_2\text{O}_2$  concentrations alone cannot substitute the need of the microbiological methods by itself. Therefore, it is preferable to incorporate an additional measurement method of the spores' viability. Different methods have been proposed to measure this, such as with optical (David L. Rosen, 1997; Tabacco and Taylor, 2000), potentiometric (Zhou et al., 2005), piezoelectric (Campbell and Mutharasan, 2006) or impedimetric sensors (Labib et al., 2012). The determination of the spores' viability generally employs additional unique biomarkers from the spore coat or byproducts from germination, for example, mRNA (messenger ribonucleic acid) (Baeumner et al., 2004), dipicolinic acid (DPA) or calcium ions ( $\text{Ca}^{2+}$ ) (Tehri et al., 2018). Therefore, specific (bio-) chemical transducers must be adapted. Nevertheless, most of these methods are solution-based, having high response times ( $> 20$  min) and are not convenient to perform under a dry gaseous environment. Recently, a novel impedimetric sensor was suggested to monitor the microbiological efficacy of gaseous  $\text{H}_2\text{O}_2$  during sterilization processes (Oberländer et al., 2018). This sensor measures the spore morphology by means of impedance changes in regard to the hydrogen peroxide concentration. It consists in a differential setup of two interdigitated electrode arrangements. On one arrangement, microbiological spores (e.g., *Bacillus atrophaeus*) are immobilized and the other one functions as a reference. The impedance of the spores is measured before and after the sterilization process and the spores' viability can be determined due to the correlation between the  $\text{H}_2\text{O}_2$  concentration and the impedance change. However, the principle of this sensor is still under ongoing research.

So far, to the extent of our knowledge, no sensor that can measure at the same time gaseous  $\text{H}_2\text{O}_2$  concentrations and can additionally evaluate the spores' viability under industrial conditions has been presented. In addition, the effect of  $\text{H}_2\text{O}_2$  on the morphology of spores has not been either investigated in detail. For these reasons, the purpose of this contribution is to develop a sensor array constructed of a calorimetric gas sensor, which can determine  $\text{H}_2\text{O}_2$  concentrations together with a spore-based biosensor, which can evaluate the spores' viability, and as a whole is able to evaluate the efficacy of the sterilization process with gaseous  $\text{H}_2\text{O}_2$  for industrial applications. Furthermore, three different spore strains, namely *Bacillus atrophaeus* DSM 675, *Bacillus subtilis* DSM 402 and *Geobacillus stearothermophilus* DSM 5934, are characterized regarding the effect of  $\text{H}_2\text{O}_2$  on them by means of impedimetric, AFM, SEM and microbiological measurements.

## 2. Materials and methods

### 2.1. Sensor fabrication: calorimetric gas- and spore-based biosensor array

The fabrication process of the sensor array was introduced in (Arreola et al., 2019). This is schematically shown in the supplementary information in Fig. S1. An adhesion promoter (Ti prime, Microchemicals GmbH, Germany) was spin-coated onto a dehydrated borosilicate glass wafer. Likewise, a positive photoresist (AZ\*5214E, Microchemicals GmbH, Germany) was deposited as well. Then, a mask aligner was used to photolithographically pattern the selected design to the photoresist (Süss MicroTec AG, Germany). Subsequently, the wafer

was developed and the metals (10 nm titanium and 100 nm platinum) were deposited by means of an e-beam evaporation process. A lift-off process (TechniStrip®Micro D350, Microchemicals GmbH, Germany) was then employed to obtain the final structures.

Moreover, the calorimetric  $\text{H}_2\text{O}_2$  sensor was fabricated according to previous investigations as shown in (Kirchner et al. 2011, 2013a; Näther et al., 2006). Briefly, the meander structures were passivated with a photoresist (SU-8, Microchemicals GmbH, Germany) to protect Pt from vaporized hydrogen peroxide. Afterwards, on the active side of the sensor,  $\text{MnO}_2$  as a catalyst was deposited.

In addition, for the spore-based biosensor, a  $10\ \mu\text{l}$  aliquot of the spore suspension (stock solution of at least  $10^8$  CFU/ml, see section 2.2 for further details) was pipetted only onto the active side of the sensor and air-dried under sterile conditions. A final spore concentration on the chip of at least  $10^6$  CFU/ml (colony forming units per milliliter) was obtained; this preparation was done in accordance to industrial requirements (Cerny, 1992). The spore concentration of  $10^6$  CFU/ml on the chip was assured during all experiments since all cleaning procedures (washing steps) were performed before spore immobilization. Both the schematic (left) and the photograph (right) of the combined sensor array can be observed in Fig. 1 a).

### 2.2. Spore production

The spore suspensions were produced according to a modified method of (Arreola et al., 2016) and performed under sterile conditions. The strains of *Bacillus subtilis* DSM 402 and *Geobacillus stearothermophilus* DSM 5934 were kindly provided from Prof. Dr. J. Bongaerts (Aachen University of Applied Sciences). The *Bacillus atrophaeus* DSM 675 strain

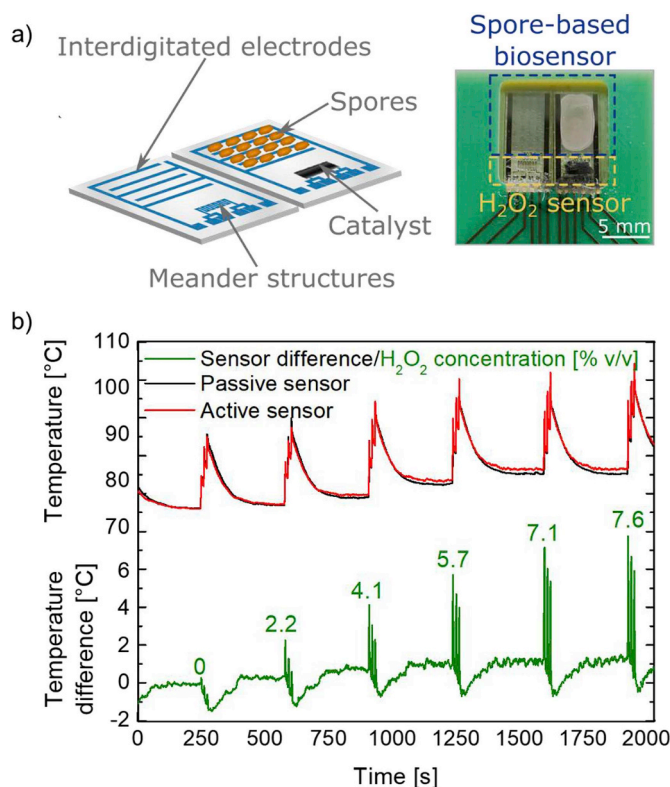


Fig. 1. a) The sensor array has a differential setup: on one sensor (active) the spores are immobilized on interdigitated electrodes and a catalyst is deposited on the meander structures, the other sensor (passive) serves as a reference. b) Calorimetric gas-sensor response to different concentrations of gaseous hydrogen peroxide. The upper curves correspond to the temperature of the catalytically active sensor and the passive one. The temperature difference and by this, the actual  $\text{H}_2\text{O}_2$  concentration is shown in the lower part curve.

was purchased from the Leibniz Institute DSMZ – German Collection of Microorganisms and Cell Cultures (Germany). All strains were cultivated with a complex medium consisting of meat extract dry (3 g/l) and peptone (5 g/l) for 24 h at 30 °C for *B. subtilis* and *B. atrophaeus*, and at 55 °C for *G. stearothermophilus*. Afterwards, the sporulation was induced by inoculation of cells on nutrient agar plates enriched with MnSO<sub>4</sub> (10 g/l) and incubated for 7 days with the above mentioned temperatures for each microorganism. Then, the spores were collected from the plates with an inoculation loop and deposited into a 15 ml centrifuge tube containing 5 ml of distilled water. The tubes were subsequently mixed by a vortex mixer and centrifuged at 4000 rpm (A-4-81; Centrifuge 5810R, Eppendorf, Germany) for 20 min at 20 °C. The vegetative cells and debris were removed from the suspension and the spores were washed with distilled water and then centrifuged again. This process was repeated at least eight times, until a spore suspension of at least 99% bacteria/debris-free was reached. Finally, to guarantee the inactivation of any remaining bacteria, the suspension was pasteurized at 80 °C for 20 min. A final concentration of 10<sup>8</sup> CFU/ml was obtained by means of serial dilutions and plating.

### 2.3. Sterilization with vaporized H<sub>2</sub>O<sub>2</sub>

All sterilization procedures were carried out in a test rig presented in (Kirchner et al., 2011; Näther et al., 2006) analog to those sterilization modules used in industrial aseptic filling machines. Here, a H<sub>2</sub>O<sub>2</sub> gas stream of 10 m<sup>3</sup>/h is provided by pressurized air used as a carrier. This air-H<sub>2</sub>O<sub>2</sub> combination is heated in a vaporizer up to 240 °C. Hydrogen peroxide concentrations can be set in the range from 0 to 7.6% v/v.

The sensor arrays were submitted to H<sub>2</sub>O<sub>2</sub> sterilization for different concentrations, namely 0, 2.2, 4.1, 5.7, 7.1 and 7.6% v/v at 240 °C for 2 s. The exposure time, the temperature and the highest H<sub>2</sub>O<sub>2</sub> concentration used in this study resemble standard parameters applied in the industry.

### 2.4. Physical and electrical characterizations

#### 2.4.1. Calorimetric H<sub>2</sub>O<sub>2</sub> sensor

Two passivated platinum meander structures were used as resistance-temperature resistors (RTDs): a change of resistance linearly varies with a change of temperature. One meander structure serves as a reference (passive sensor), whereas the other one as a sensing element (active sensor); the passive sensor remains inert to H<sub>2</sub>O<sub>2</sub> while on the active sensor, MnO<sub>2</sub> catalyzes H<sub>2</sub>O<sub>2</sub>. As a result, an increase of temperature occurs on the active sensor and a temperature difference between both sensors can be correlated to the hydrogen peroxide concentration. Furthermore, a water bath thermostat (Omnicoil, LAUDA Scientific GmbH, Germany) was used to temperature-calibrate them from 0 to 80 °C in 10 °C steps. In addition, the four-point probe method was used to measure the resistance of the sensors and it was recorded using a data acquisition card (USB-9219, National Instruments Corporation, United States) and a built-in LabView program. At least four sensors were used for each hydrogen peroxide concentration and spore strain.

#### 2.4.2. Spore-based biosensor

The viability of the spores was measured by means of impedimetric measurements. For this, a precision LCR meter (E4980A, Agilent Technologies, United States) was utilized with a fixed frequency of 3 kHz and an excitation voltage of 20 mV with a direct current voltage bias of 0 V. The direct current bias of 0 V was carefully chosen according to typically used literature values for similar impedance spectroscopy measurements with interdigitated electrodes in combination with microorganisms (Mallén-Alberdi et al., 2016; Rosati et al., 2019). Furthermore, the OCP was not measured, since we do not use any external reference electrode or measure in solution during our experiments. Nevertheless, stability investigations of the interdigitated structures have been made showing no effect from gaseous hydrogen peroxide on them

or any other described process steps (Oberländer et al., 2015). In addition, to assure a reliable sensor signal, we implemented a differential setup, where one sensor serves as a reference and the other as sensing element (e.g., catalytically activated or with spores).

Moreover, to be able to analyze between different sensors, the sensor impedance was normalized by the following equation (Eq. (2)):

$$\text{Normalized impedance (\%)} = \left( \frac{\text{Blank sensor} - \text{Procedure}}{\text{Blank sensor}} \right) \times 100 \quad (2)$$

*Blank sensor* connotes the measurement of the sensor without spores and *Procedure*, the impedance change after the spores were confined onto the IDEs, and sterilized with different hydrogen peroxide concentrations (see section 2.3). At least four sensors were used for each H<sub>2</sub>O<sub>2</sub> concentration.

#### 2.4.3. Scanning electron microscopy (SEM)

A scanning electron microscope (JSM-7800F, JEOL Ltd., Japan) was employed to study the morphology of the spores after sterilization with H<sub>2</sub>O<sub>2</sub>. For these measurements, the samples were prepared by sputtering a 10 nm layer of Pt/Pd (80:20) on them.

Moreover, qualitative evaluations were performed by classifying the spores in different types, namely “normal”, “deformed” and “flattened”. For each hydrogen peroxide concentration, the ratio of the particular spore type was determined by counting them manually; this was performed at least three times. 1551 to 3440 spores were counted and evaluated for each spore strain.

#### 2.4.4. Atomic force microscopy (AFM)

A more quantitative investigation (height measurements) to study the morphology of spores after being treated with H<sub>2</sub>O<sub>2</sub> was conducted utilizing an atomic force microscope (BioMat Workstation, JPK Instruments, Germany). Here, silicon probes (Arrow NCR, NanoWorld AG, Switzerland) were operated with a force constant of 42 N/m and a resonance frequency of 285 kHz. All the recordings (20 × 20 μm<sup>2</sup>) were carried out in tapping mode at 512 pixels per line with a scanning frequency of 0.6 Hz under environmental conditions. Moreover, an open-source software (Gwyddion, <http://gwyddion.net/>) was used to visualize and analyze the height measurement of the spores; this was obtained by measuring the average height of each spore, i.e., no cross section tool was used, but a mask for the whole spore.

## 3. Results and discussion

### 3.1. Calorimetric H<sub>2</sub>O<sub>2</sub> sensor

H<sub>2</sub>O<sub>2</sub> concentrations between 0 and 7.6% v/v were determined within 2 s by means of a calorimetric H<sub>2</sub>O<sub>2</sub> sensor as shown in Fig. 1 b). On the upper part of the graph, the temperatures of both active and passive sensors can be observed. Furthermore, their temperature difference and the hydrogen peroxide concentration are shown on the bottom part. Taken 0% v/v H<sub>2</sub>O<sub>2</sub> as a reference, no distinguishable temperature difference was observed during the resting phase (no exposure). However, for all other concentrations, as the H<sub>2</sub>O<sub>2</sub> concentration rises, a higher exothermic reaction takes place on the active sensor part than the passive one and the temperature difference between them increases. As a result, a sensor sensitivity of 0.97 °C/(% v/v) was obtained. This sensitivity is lower than that found in literature by polyimide sensors (2.06 °C/(% v/v) (Kirchner et al., 2013b)). The reason for that is due to the fact that polyimide films have a lower thermal conductivity (0.16 W/mK) than borosilicate glass substrates (1.2 W/mK). Thus, it may reduce thermal flow (Wheeler et al., 2001) generated on the active sensor and hence increase the temperature difference between sensors, i.e., enhancing the sensitivity. Additionally, three characteristic peaks (Kirchner et al., 2013b) can be seen along all H<sub>2</sub>O<sub>2</sub> concentrations, which correspond to the 2 s response time of the sensor; the precise measurement of H<sub>2</sub>O<sub>2</sub> concentrations up to 7.6% v/v

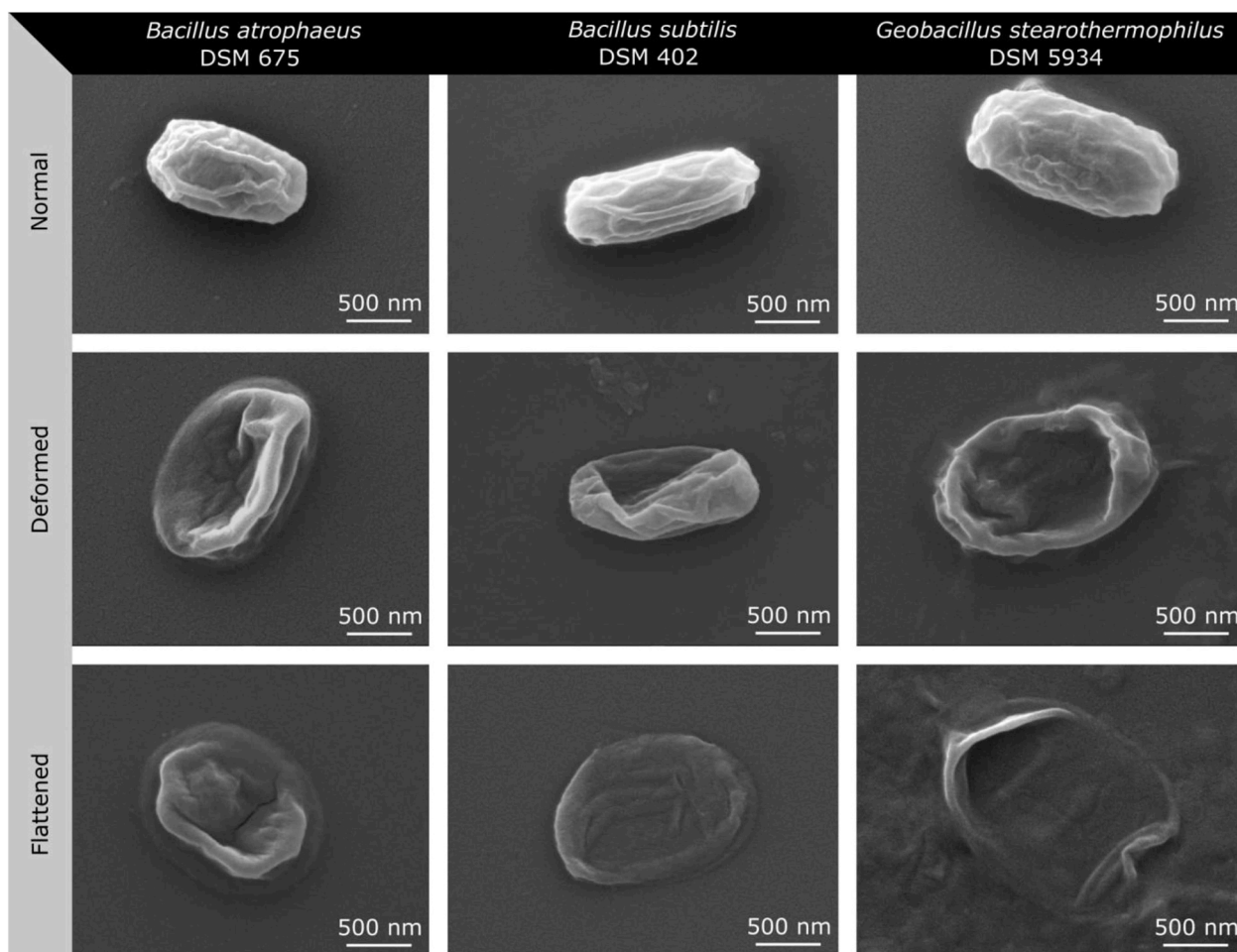


Fig. 2. SEM pictures of representative morphology types of *Bacillus atrophaeus* DSM 675, *Bacillus subtilis* DSM 402 and *Geobacillus stearothermophilus* DSM 5934 spores commonly encountered as: “normal”, “deformed” and “flattened”. The flattened type was found only after  $H_2O_2$  sterilization.

(a typical concentration in industrial applications) within 2 s was successfully demonstrated. Further magnification of the peaks and the calibration curve of the sensor can be found in Fig. S2 a) and b) from the supplementary section.

### 3.2. Effect of gaseous $H_2O_2$ on the morphology of spores

#### 3.2.1. SEM measurements

Different spore suspensions of *B. subtilis*, *B. atrophaeus* and *G. stearothermophilus* were physically characterized by SEM measurements after exposure to various  $H_2O_2$  concentrations to analyze morphological changes of spores. Several morphology conditions of spores could be differentiated for each strain: depending on the spore status the spores were labeled as “normal”, “deformed” or “flattened” as shown in Fig. 2. The normal and deformed conditions were encountered in a specific ratio, which varies, depending on the applied  $H_2O_2$  gas concentration. In contrast, the flattened condition was only found after treating the spores with gaseous hydrogen peroxide. The ratio of such conditions was evaluated by SEM in Fig. 3a) and b) and c), as stated in section 2.4.3. For the evaluation of the data between 1551 and 3440 spore samples have been investigated each, to guarantee statistically relevant data. As it can be seen for *B. atrophaeus* (Fig. 3 a)), at the beginning of the sterilization process (0% v/v  $H_2O_2$ ) 77.76%  $\pm$  2.04% were normal spores and 22.23%  $\pm$  2.04% deformed spores; no flattened spores were found at this stage. As the  $H_2O_2$  concentration was increased, the amount of normal spores decreased (the only exception was 5.7% v/v  $H_2O_2$ ), and that of the deformed- and flattened spores increased. During the maximum concentration of 7.6% v/v  $H_2O_2$ , 38.97%  $\pm$  2.49% of normal-, 27.77%  $\pm$  3.48% deformed- and

33.25%  $\pm$  0.98% flattened spores were found. Moreover, for *B. subtilis* (Fig. 3 b)), without  $H_2O_2$  exposure the flattened spore type was practically absent with a value of 0.97%  $\pm$  0.41%, following by 30.94%  $\pm$  5.59% of deformed- and 68.07%  $\pm$  5.57% of normal spores. For concentrations higher than 5.7% v/v  $H_2O_2$  no significant further decrease of the flattened spores was observed. However, a decrease of the normal spores as well as an increase of the deformed spores can be seen for the last two concentrations of 7.1 and 7.6% v/v  $H_2O_2$ . As an example, the distributions at 7.6% v/v for normal-, deformed- and flattened spores were 47.46%  $\pm$  5.98%, 36.97%  $\pm$  0.74%, 15.56%  $\pm$  5.23%, accordingly. Furthermore, in the case of *G. stearothermophilus* (Fig. 3 c)), it can be noted that the proportion of the spore types along the  $H_2O_2$  concentrations changed significantly after the first dosage (2.2% v/v  $H_2O_2$ ), where the presence of normal spores decreased and the deformed- and flattened spores dramatically increased. Further concentrations from 4.1% v/v  $H_2O_2$  onwards did not notably influence the spore condition distribution, except for the last concentration of 7.6% v/v, where the flattened spores increased and the deformed- and normal spores decreased with final values of 35.50%  $\pm$  8.86%, 13.52%  $\pm$  4.63% and 50.97%  $\pm$  5.93%, respectively.

Besides the morphology change of spores due to hydrogen peroxide, other parameters may also intervene in the structure modification of the spores such as the sample preparation (sputtering of metal on spores) or vacuum during the SEM measurement. For this reason, the spores were further evaluated by means of AFM.

#### 3.2.2. AFM measurements

The effect of hydrogen peroxide on different spores was additionally quantitatively evaluated by means of AFM. Firstly, the height of each

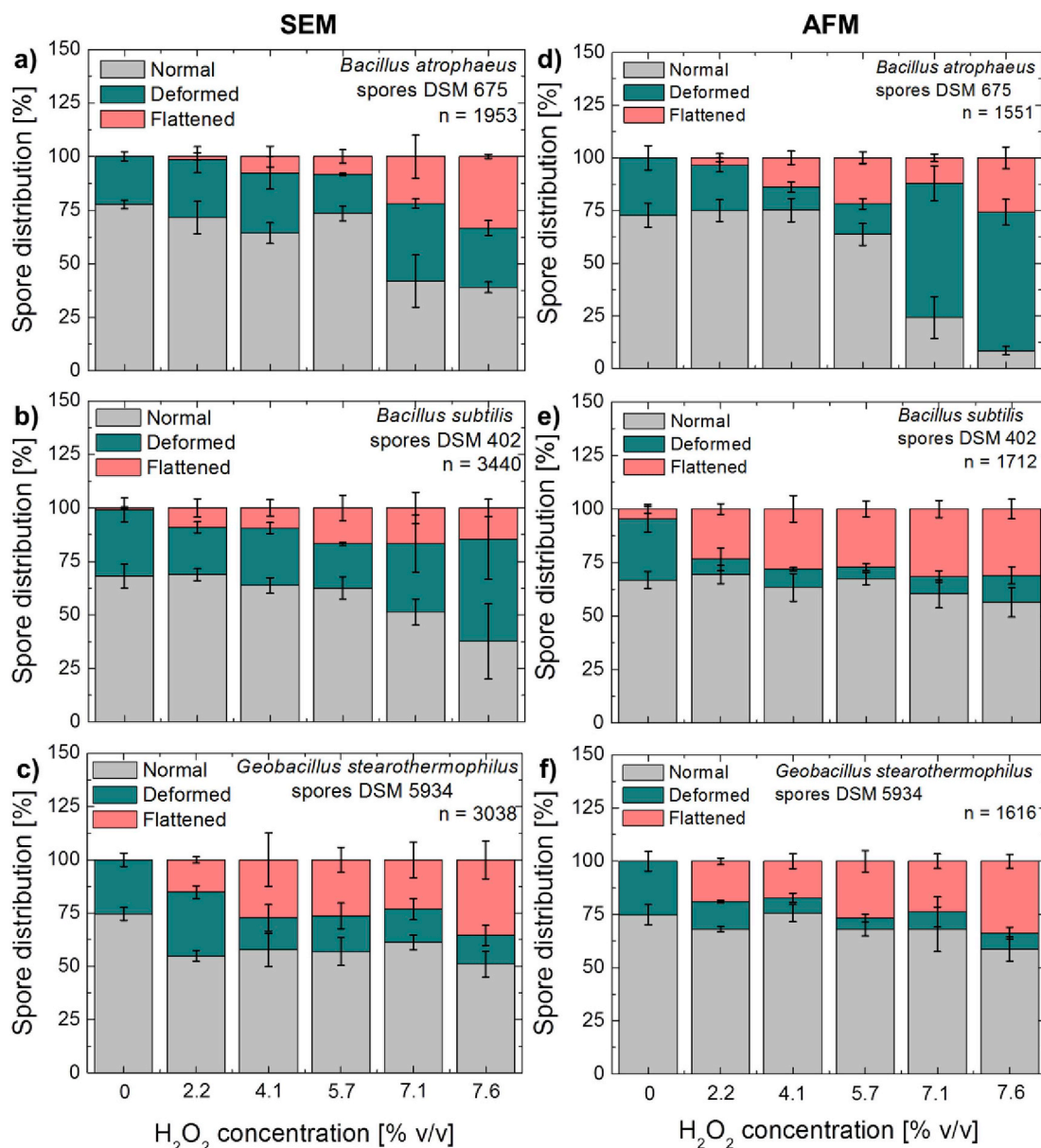


Fig. 3. Comparison of SEM (a, b) and c) vs. AFM measurements (d, e) and f) regarding the distribution of different spore conditions (“normal”, “deformed”, “flattened”) from *Bacillus atropheus* DSM 675 (top), *Bacillus subtilis* DSM 402 (middle) and *Geobacillus stearothermophilus* DSM 5934 (bottom) after being treated with gaseous hydrogen peroxide. For each presented graph “n” spores were investigated for all shown concentrations.

spore category (“normal”, “deformed” and “flattened”) was determined (Table 1), even though the spore-size values vary depending on the preparation and measurement techniques of the spores (Carrera et al., 2007). To each value 520 spores have been investigated, in our case, under normal conditions, *G. stearothermophilus* possesses the highest height of all of them. Meanwhile *B. atropheus* and *B. subtilis* retain similar values. During the deformed condition, *B. subtilis* and *G. stearothermophilus* share similar heights, whereas *B. atropheus* displays the lowest height in this form. Lastly, similar heights of all spores can be seen in the flattened case. It is also worthy to note that those height values do not significantly change along  $H_2O_2$  concentrations, but the ratio of the different spore conditions does. For example, a normal spore encountered at 0% v/v  $H_2O_2$  has a comparable height value as a normal spore encountered at 7.6% v/v  $H_2O_2$ ; the same is also true for the other spore conditions.

Moreover, to corroborate the SEMs measurements from the last section, the spores were treated with the same conditions as before: they were exposed to different hydrogen peroxide concentrations.

Table 1

Height measurements (nm) of *B. atropheus*, *B. subtilis* and *G. stearothermophilus* spores (to each value in table 520 spores have been investigated).

Spore condition	<i>B. atropheus</i>	<i>B. subtilis</i>	<i>G. stearothermophilus</i>
“Normal”	530.05 ± 120.31	540.35 ± 96.97	671.19 ± 119.15
“Deformed”	375.00 ± 85.30	437.00 ± 83.09	441.36 ± 122.98
“Flattened”	241.36 ± 68.38	239.67 ± 77.68	242.57 ± 81.49

Later, they were qualitatively (spore distribution) and quantitatively (spore height) assessed. From Fig. 3d) and e) and f) similar results can be observed after sterilization with  $H_2O_2$ . Without hydrogen peroxide, both SEM and AFM are in a good agreement, probably suggesting no additional effect from the SEM measurements to the morphology of the spores at this stage. Furthermore, from the  $H_2O_2$  concentration of 2.2% v/v onwards, differences are appreciable; particularly, this has been found for the last two concentrations (7.1 and 7.6% v/v  $H_2O_2$ ) of *B. subtilis* and *B. atropheus*, where the amount of normal- and deformed

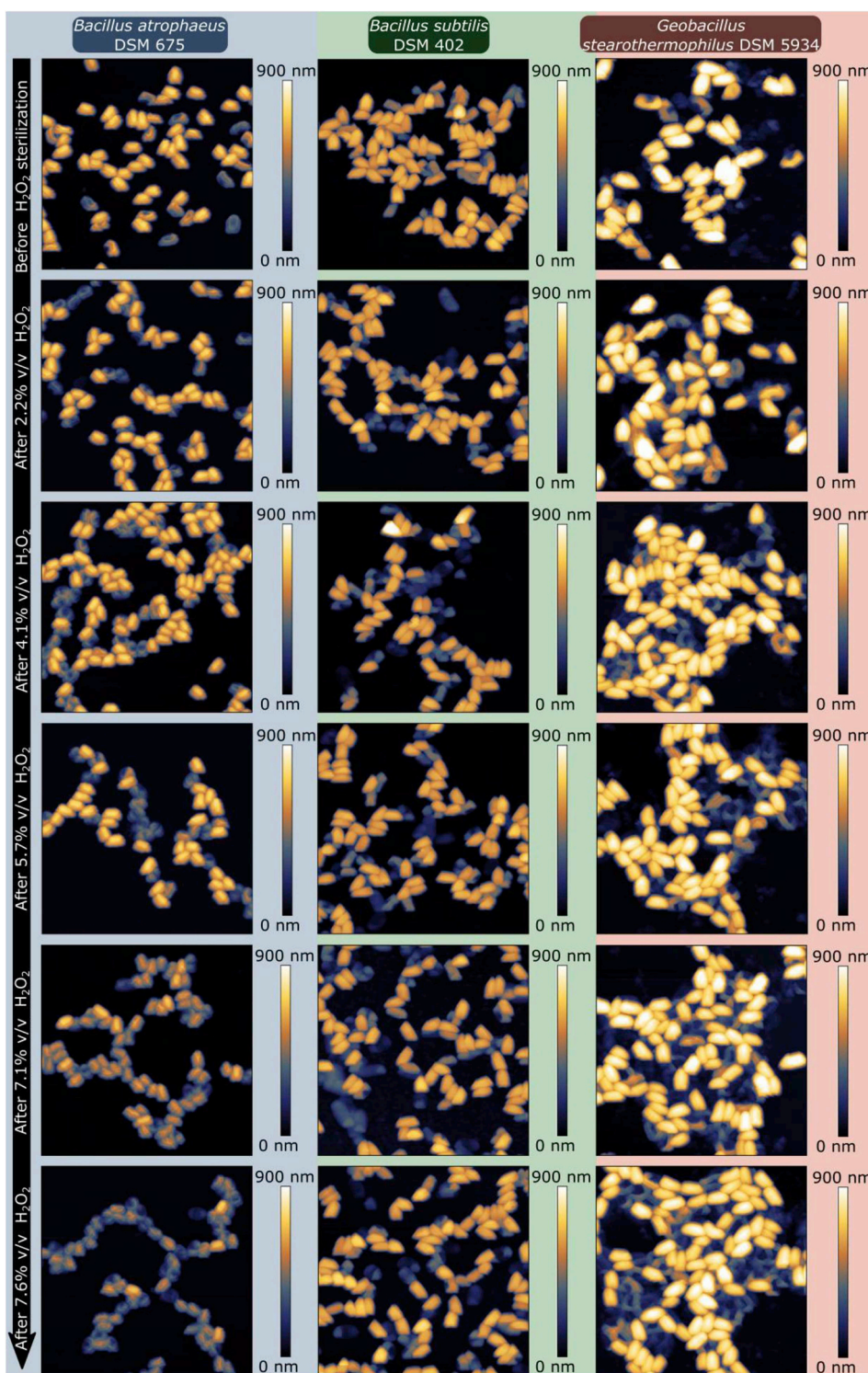


Fig. 4. AFM measurements ( $20 \times 20 \mu\text{m}^2$ ) of *Bacillus atropheus* DSM 675 (left), *Bacillus subtilis* DSM 402 (middle) and *Geobacillus stearothermophilus* DSM 5934 (right) spores sterilized with different concentrations of H<sub>2</sub>O<sub>2</sub> (0–7.6% v/v from top to bottom).

spores deviates from than that of the SEM. Nonetheless, both characterization methods show similar tendency.

Besides the different conditions, the respective averaged spore height of all three types of factors (average of all conditions weighted by the distribution of different spore conditions from Fig. 3d) and e) and f)) was determined (Fig. 4) and evaluated (Fig. 5 a)) for each H<sub>2</sub>O<sub>2</sub> concentration. As it can be seen for *B. atropheus*, at the beginning of the sterilization test series (0% v/v H<sub>2</sub>O<sub>2</sub>) the average height of all spore categories was  $463.4 \text{ nm} \pm 129.05 \text{ nm}$ . During the maximum

concentration of 7.6% v/v H<sub>2</sub>O<sub>2</sub>, the average spore height was  $288.99 \text{ nm} \pm 134.96 \text{ nm}$ . Moreover, for *B. subtilis* after 2.2% v/v H<sub>2</sub>O<sub>2</sub> concentration, no further significant decrease of the average height of the spores was observed. At the end of the sterilization process, the average height was  $409.68 \text{ nm} \pm 162.66 \text{ nm}$ . As comparison, for the 0% v/v H<sub>2</sub>O<sub>2</sub> concentration, the spores' height was  $460.29 \text{ nm} \pm 168.35 \text{ nm}$ . Furthermore, for *G. stearothermophilus* no significant average height change was observed; it was nearly constant for all H<sub>2</sub>O<sub>2</sub> concentrations.

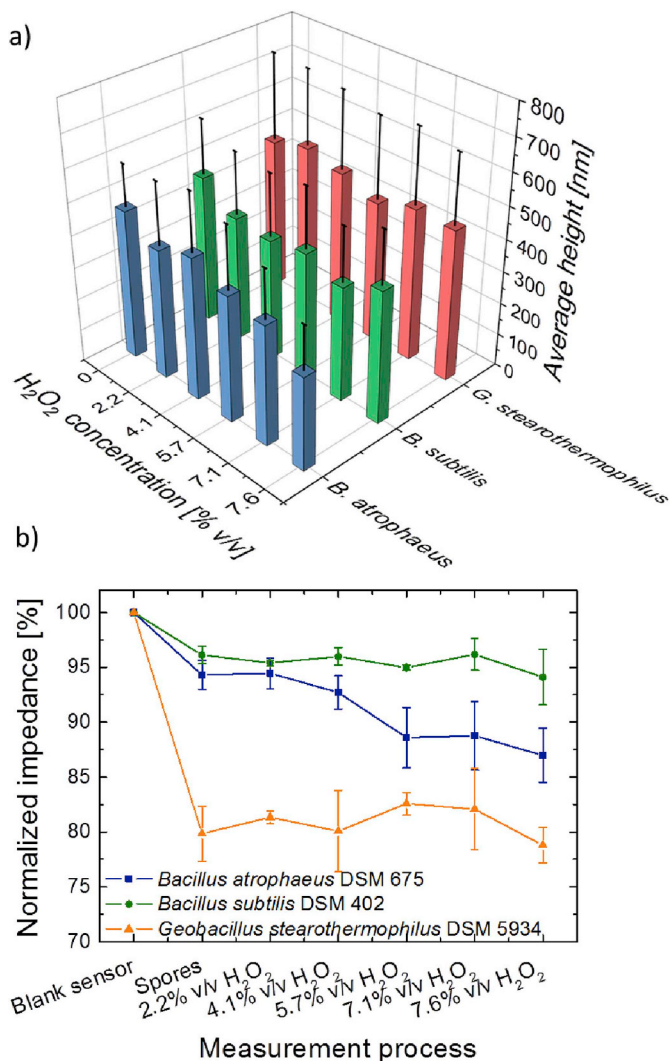


Fig. 5. a) Averaged spore-height measurements of *Bacillus atrophaeus* DSM 675, *Bacillus subtilis* DSM 402 and *Geobacillus stearothermophilus* DSM 5934 spores for different concentrations of hydrogen peroxide. b) Signal response (impedance) of spore-based biosensors. The sensors were measured at different stages (at least four sensors were used for each step). In the first stage, the sensors were measured after being cleaned. In the second step, *Bacillus atrophaeus* DSM 675, *Bacillus subtilis* DSM 402 and *Geobacillus stearothermophilus* DSM 5934 spores were immobilized on them. Subsequently, in the following stages, the spore-based biosensors were submitted to several concentrations of gaseous hydrogen peroxide.

In summary, H<sub>2</sub>O<sub>2</sub> influences in a different manner each spore strain. The decreases of height and of the spore conditions of *B. atrophaeus* spores have a relatively linear relationship to the increase of H<sub>2</sub>O<sub>2</sub> concentration. In addition, the height of spores of *B. subtilis* after being exposed to the minimal concentration (in our case 2.2% v/v H<sub>2</sub>O<sub>2</sub>) remains practically constant, whereas the normal- and deformed spores linearly decrease, but the flattened spores prevail in a steady behavior. For *G. stearothermophilus*, the spores' height is fairly maintained during all hydrogen peroxide concentrations. Moreover, after the first exposure to H<sub>2</sub>O<sub>2</sub>, the normal proportion of spores decreased and the deformed spores notably increased. From this step on until the penultimate concentration (7.1% v/v H<sub>2</sub>O<sub>2</sub>), the spores' height as well as the different spore types stayed at a constant state.

The relationship between H<sub>2</sub>O<sub>2</sub> concentration and the spore morphology (different spore conditions and spore height) is a decisive parameter to shed light on further development on this novel type of spore-based biosensors applied in industrial processes. For example, from the AFM and SEM measurements, it has been realized that not all

spore strains may be optimal candidates for a spore-based biosensor used to assure a proper functioning of aseptic machines, since the spore-coat sensitivity to gaseous hydrogen peroxide of each varies.

So far, the impact of H<sub>2</sub>O<sub>2</sub> on spores by means of morphological changes has been investigated. One step further is to examine the relationship between these morphological- and sensor-signal changes (impedance) from spore-based biosensors (see section 3.3).

### 3.3. Spore-based biosensor

The different spore types, namely *B. atrophaeus*, *B. subtilis* and *G. stearothermophilus* (see section 2.2), were simultaneously characterized by means of impedimetric measurements. Fig. 5 b) depicts the respective normalized sensor signal at different stages of the measurement process, including a reference step (blank sensor), the electrical properties of the spores after immobilization onto the sensor surface (spores) and the effect of different concentrations of H<sub>2</sub>O<sub>2</sub> peroxide (2.2–7.6% v/v) on the spores, measured at the same time with the H<sub>2</sub>O<sub>2</sub> calorimetric sensor from section 3.1. As it is noticeable from the graph, after immobilizing the spores on the sensor surface, *G. stearothermophilus* has the highest sensor-signal change (impedance) to 79.84% ± 2.5% from the starting value of 100% compared to the other *Bacillus* species, particularly 96.12% ± 0.8% for *B. subtilis* and 94.03% ± 1.31% for *B. atrophaeus*. Furthermore, most of them do not show a linear behavior to the increment of H<sub>2</sub>O<sub>2</sub> concentrations (except for *B. atrophaeus*). *B. subtilis* and *G. stearothermophilus* exhibit an irregular flat performance; however, for all the cases the impedance change at the highest concentration (7.6% v/v) could underline a measurable impedance change for typical concentrations applied in industrial processes. The highest impedance change at this concentration for *B. atrophaeus* was 7.05%, followed by *B. subtilis* with 2.02% and finally, *G. stearothermophilus* with 1.05%. In case of *B. atrophaeus* as a test organism, the spore-based biosensor is able to distinguish between all investigated concentrations. For *B. subtilis* and *G. stearothermophilus* this is still true but limited only to the highest hydrogen peroxide concentration (7.6% v/v).

Moreover, it has been suggested in literature (Oberländer et al., 2018) that the change of impedance after sterilization with gaseous H<sub>2</sub>O<sub>2</sub> can be related to a morphological change of the spores. This correlation of the morphological change has been similarly reported for other sterilization techniques, such as spores treated with metal oxide nanoparticles (Stoimenov et al., 2002), surfactants (Pinzon-Arango et al., 2009) or plasma treatment (Tarasenko et al., 2006). However, the opposite has been discussed in literature as well: no morphological change after a sterilization process, for example, by treating the spores with electrical discharges (Lamarche et al., 2018). In our case, as reviewed in the previous section, H<sub>2</sub>O<sub>2</sub> indeed induced a morphology change on all investigated spores. Therefore, the impedance change from the spore-based biosensor is likely to occur due to the transition to different spores conditions. As the spores change from the deformed to flattened condition, they may start leaking cell constituents, making the sensor surface more conductive and thus reducing its overall impedance (Oberländer et al., 2018). As a result, the morphology change of the spores is suitable as a physical parameter to determine the spores' viability.

### 4. Conclusions

In this work, a combined sensor array consisting of a calorimetric gas- and a spore-based biosensor for online monitoring of sterilization processes with gaseous H<sub>2</sub>O<sub>2</sub> under industrial conditions was introduced for the first time. H<sub>2</sub>O<sub>2</sub> concentrations up to 7.6% v/v were determined with a sensor sensitivity of 0.97 °C/(% v/v). Furthermore, the effect of H<sub>2</sub>O<sub>2</sub> on different spore strains namely, *Bacillus atrophaeus* DSM 675, *Bacillus subtilis* DSM 402 and *Geobacillus stearothermophilus* DSM 5934, were meticulously investigated by means of SEM, AFM and impedimetric measurements. Every spore strain was differently affected by H<sub>2</sub>O<sub>2</sub>. Three spore categories were identified during the

sterilization process and eventually transitioned from one to the next condition: “normal”, “deformed” and “flattened”. The average spores' height of *B. atrophaeus* showed a fairly linear correlation to the H<sub>2</sub>O<sub>2</sub> concentration. Meanwhile, *B. subtilis* spores showed a rapid decrement of their height after 2.2% v/v H<sub>2</sub>O<sub>2</sub>, whereas *G. stearothermophilus* showed a steady height along all H<sub>2</sub>O<sub>2</sub> concentrations. In addition, the efficacy of a sterilization process with gaseous H<sub>2</sub>O<sub>2</sub> was carried out with a spore-based biosensor. Sensors fabricated with *B. atrophaeus* were able to successfully distinguish between all investigated H<sub>2</sub>O<sub>2</sub> concentrations. Spores from *B. subtilis*, and *G. stearothermophilus* were still able to evaluate qualitatively the sterilization process but limited to the H<sub>2</sub>O<sub>2</sub> concentration of 7.6% v/v. Nevertheless, it was shown as well that the sensor's signal is likely due to the morphology change of the spores; specifically, the transition to the different spores' conditions and this parameter is convenient to determine the viability of the spores.

The presented combined sensor array consisting of a gaseous hydrogen peroxide sensor that benefits from a quick response time (2 s) and a spore-based biosensor, which enables measuring impedance changes due to morphological variation of spore size, opens unique approaches regarding evaluation and monitoring of sterilization processes with H<sub>2</sub>O<sub>2</sub> in aseptic food industry. Hydrogen peroxide concentrations can be precisely measured within industrial operation conditions. This provides several advantages such as online- and inline monitoring, ease of portability (miniaturized system) and no further sample preparation is needed. Additionally, the efficacy of the sterilization process can be effectively determined by the embedded spore-based biosensor. This work demonstrated that *Bacillus atrophaeus* spores can be used for quantitative determination and the other investigated strains (*B. subtilis* and *G. stearothermophilus*) showed restricted correlation between morphological- and impedance changes while being exposed to hydrogen peroxide. The synergy of the two sensor types as one combined sensor array allows a considerably more specific multi-parameter experience in aseptic filling machines in comparison to isolated microbiological state-of-the-art- or hydrogen peroxide methods.

Further investigations will focus on the increase of the sensor's sensitivity of the calorimetric gas- and spore-based biosensors by employing substrates with lower thermal coefficients (e.g., polyimide films) or optimizing the spore number and immobilization techniques on the biosensor array.

#### CRediT authorship contribution statement

**Julio Arreola:** Conceptualization, Methodology, Software, Validation, Formal analysis, Investigation, Resources, Writing - original draft, Writing - review & editing, Visualization, Project administration. **Michael Keusgen:** Conceptualization, Methodology, Investigation, Writing - original draft, Writing - review & editing, Supervision. **Torsten Wagner:** Conceptualization, Methodology, Investigation, Writing - original draft, Writing - review & editing, Supervision, Project administration, Funding acquisition. **Michael J. Schöning:** Conceptualization, Methodology, Investigation, Writing - original draft, Writing - review & editing, Supervision, Project administration, Funding acquisition.

#### Declaration of competing interest

The authors declare that they have no known competing financial interests or personal relationships that could have appeared to influence the work reported in this paper.

#### Acknowledgements

The authors are thankful to Prof. Dr. P. Siegert and Prof. Dr. J. Bongaerts for access to the microbiology laboratory for microbiological

research, H. Iken and J. Oberländer for support during the fabrication of the sensor array and D. Rolka for the SEM measurements. The financial funds were provided by the Federal Ministry of Education and Research, Germany, Project: “SteriSens” (Fund. No.: 03FH057PX5).

#### Appendix A. Supplementary data

Supplementary data to this article can be found online at <https://doi.org/10.1016/j.bios.2019.111628>.

#### References

- Ansari, I.A., Datta, A.K., 2003. Food Bioprod. Process. 81 (1), 57–65.
- Arreola, J., Keusgen, M., Schöning, M.J., 2019. Electrochim. Acta (302), 394–401.
- Arreola, J., Mätzkow, M., Durán, M.P., Greeff, A., Keusgen, M., Schöning, M.J., 2016. Phys. Status Solidi A 213 (6), 1463–1470.
- Baemmer, A.J., Leonard, B., McElwee, J., Montagna, R.A., 2004. Anal. Bioanal. Chem. 380 (1), 15–23.
- Campbell, G.A., Mutharasan, R., 2006. Biosens. Bioelectron. 21 (9), 1684–1692.
- Carrera, M., Zandomeni, R.O., Fitzgibbon, J., Sagripanti, J.-L., 2007. J. Appl. Microbiol. 102 (2), 303–312.
- Cerny, G., 1992. Packag. Technol. Sci. 5 (2), 77–81.
- Heckert, R.A., Best, M., Jordan, L.T., Dulac, G.C., Eddington, D.L., Sterritt, W.G., 1997. Appl. Environ. Microbiol. 63 (10), 3916–3918.
- Johnston, M.D., Lawson, S., Otter, J.A., 2005. J. Microbiol. Methods 60 (3), 403–411.
- Kirchner, P., Li, B., Spelthahn, H., Henkel, H., Schneider, A., Friedrich, P., Kolstad, J., Keusgen, M., Schöning, M.J., 2011. Sens. Actuators B Chem. 154 (2), 257–263.
- Kirchner, P., Oberländer, J., Suso, H.-P., Rysstad, G., Keusgen, M., Schöning, M.J., 2013a. Food Control 31 (2), 530–538.
- Kirchner, P., Oberländer, J., Suso, H.-P., Rysstad, G., Keusgen, M., Schöning, M.J., 2013b. Phys. Status Solidi A 210 (5), 877–883.
- Kitancharoen, N., Yamamoto, A., Hatai, K., 1997. Mycoscience 38 (4), 375–378.
- Koda, S., Kumagai, S., Ohara, H., 1999. Acta Med. Okayama 53 (5), 217–223.
- Kulyts, J., 1992. Sens. Actuators B Chem. 9 (2), 143–147.
- Labib, M., Zamay, A.S., Kolovskaya, O.S., Reshetneva, I.T., Zamay, G.S., Kibbee, R.J., Sattar, S.A., Zamay, T.N., Berezovski, M.V., 2012. Anal. Chem. 84 (21), 8966–8969.
- Lamarche, C., Da Silva, C., Demol, G., Dague, E., Rols, M.-P., Pillet, F., 2018. PLoS One 13 (8) e0201448 (1–15).
- Liu, S., Sun, H., Nagarajan, R., Kumar, J., Gu, Z., Cho, J., Kurup, P., 2011. Sensor Actuat. A-Phys. 167 (1), 8–13.
- Mallén-Alberdi, M., Vigués, N., Mas, J., Fernández-Sánchez, C., Baldi, A., 2016. Sens. Biosensing Res. 7, 100–106.
- Näther, N., Henkel, H., Schneider, A., Schöning, M.J., 2009. Phys. Status Solidi A 206 (3), 449–454.
- Näther, N., Juárez, L.M., Emmerich, R., Berger, J., Friedrich, P., Schöning, M.J., 2006. Sensors 6 (4), 308–317.
- Oberländer, J., Bromm, A., Wendeler, L., Iken, H., Durán, M.P., Greeff, A., Kirchner, P., Keusgen, M., Schöning, M.J., 2015. Phys. Status Solidi A 212 (6), 1299–1305.
- Oberländer, J., Kirchner, P., Boyen, H.-G., Schöning, M.J., 2014. Phys. Status Solidi A 211 (6), 1372–1376.
- Oberländer, J., Mayer, M., Greeff, A., Keusgen, M., Schöning, M.J., 2018. Biosens. Bioelectron. 104, 87–94.
- Otter, J.A., French, G.L., 2009. J. Clin. Microbiol. 47 (1), 205–207.
- Pinzon-Arango, P.A., Scholl, G., Nagarajan, R., Mello, C.M., Camesano, T.A., 2009. J. Mol. Recognit. 22 (5), 373–379.
- Rosati, G., Cunego, A., Fracchetti, F., Del Casale, A., Scaramuzza, M., Toni, A. de, Torriani, S., Paccagnella, A., 2019. Chemosensors 7 (1), 8.
- Rosen, D.L., 1997. Bacterial Spore Detection and Quantification Methods (5876960).
- Stoimenov, P.K., Klinger, R.L., Marchin, G.L., Klabunde, K.J., 2002. Langmuir 18 (17), 6679–6686.
- Swartling, P., Lindgren, B., 1968. J. Dairy Res. 35 (03), 423–428.
- Tabacco, M.B., Taylor, L.C., 2000. Optical Sensors for Rapid, Sensitive Detection and Quantitation of Bacterial Spores (6498041 B1).
- Tarasenko, O., Nourbakhsh, S., Kuo, S.P., Bakhtina, A., Alusta, P., Kudasheva, D., Cowman, M., Levon, K., 2006. IEEE Plasma Sci 34 (4), 1281–1289.
- Tehri, N., Kumar, N., Raghu, H.V., Vashishth, A., 2018. Ann. Microbiol. 68 (9), 513–523.
- Toledo, R.T., 1988. Overview of sterilization methods for aseptic packaging materials. In: Hotchkiss, J.H. (Ed.), Food and Packaging Interactions: Developed from a Symposium Sponsored by the Division of Agricultural and Food Chemistry at the 193<sup>rd</sup> Meeting of the American Chemical Society, Denver, Colorado, April 5–10, 1987. American Chemical Society, Washington, DC, USA, pp. 94–105.
- Verma, A.L., Saxena, S., Saini, G.S.S., Gaur, V., Jain, V.K., 2011. Thin Solid Films 519 (22), 8144–8148.
- Wheeler, M.C., Tiffany, J.E., Walton, R.M., Cavicchi, R.E., Semancik, S., 2001. Sens. Actuators B Chem. 77 (1–2), 167–176.
- Xu, M., Bunes, B.R., Zang, L., 2011. ACS Appl. Mater. Interfaces 3 (3), 642–647.
- Zhou, Y., Yu, B., Levon, K., 2005. Biosens. Bioelectron. 20 (9), 1851–1855.